Nonlinear Dynamics **10:** 19–30, 1996.

A Numerical Method for Determining Nonlinear Normal Modes

JOSEPH C. SLATER
Department of Mechanical and Materials Engineering, Wright State University, Dayton, OH 45435, U.S.A.

(Received: 15 April 1994; accepted: 17 April 1995)

Abstract. This paper examines a new approach for determining the nonlinear normal modes of undamped non-gyroscopic multiple degree-of-freedom systems. Unlike algebraic solutions that generally assume a solution in the form of a polynomial expansion, this method makes only the assumption of repetitive motion in numerically determining the mode shapes. The advantage of this approach is that the accuracy obtained in the mode shape identification is a function only of the accuracy of the numerical integration used and not of the number of terms in the power series expansion. The drawbacks are that invariance of the modal manifolds cannot be proven and mode bifurcations can be easily overlooked.

Key words: Nonlinear models, nonlinear dynamics, numerical methods.

Introduction

This work presents a new way of considering and determining nonlinear normal modes for discrete nonlinear system models. This concept has been approached by numerous authors since the original defining work of Rosenberg in 1966 [7]. The thesis of Vakakis [12] demonstrates the perturbation methodology of Manevich and Mikhlin [4] as well as the method of multiple scales [5] for finding nonlinear normal modes. An invariant manifold method for identifying nonlinear normal modes and their corresponding modal equations has been demonstrated by Shaw and Pierre [9]. Nonlinear normal modes have been determined numerically by Vakakis [12] by "observing the simulated oscillation in the configuration plane of the system" for various modal amplitudes. This paper demonstrates that the accuracy of perturbation methods breaks down for higher amplitudes.

Rosenberg [7] defined normal modes as "Vibrations-in-unison of an admissible, autonomous system." Shaw and Pierre [9] have shown that this definition is too restrictive in that it does not account for motion in which the phase of the motion varies as a function of location in the structure. Shaw and Pierre [10, 11] and Shaw [8] further extended their method to two distinct methods for finding nonlinear normal modes of distributed parameter models. These two methods are compared in Boivin *et al.* [1].

King and Vakakis [3] have developed an energy based method for finding nonlinear normal modes of undamped systems, and Nayfeh and Nayfeh [6] have demonstrated the application of the Method of Multiple Scales for finding nonlinear normal modes. Vakakis and Cetinkaya [13] have demonstrated the existence of nonlinear mode localization in perfectly symmetric, weakly coupled structures. Caughey *et al.* [2] investigated bifurcations of normal modes for different forms of stiffness nonlinearities and Vakakis and Rand [14, 15] used Poincaré maps to examine bifurcation at low energies and chaotic motion at high energies.

In what follows, the nonlinear normal mode definitions of Rosenberg [7] are applied to a set of weakly nonlinear equations representing a simple nonlinear system. This restricts the

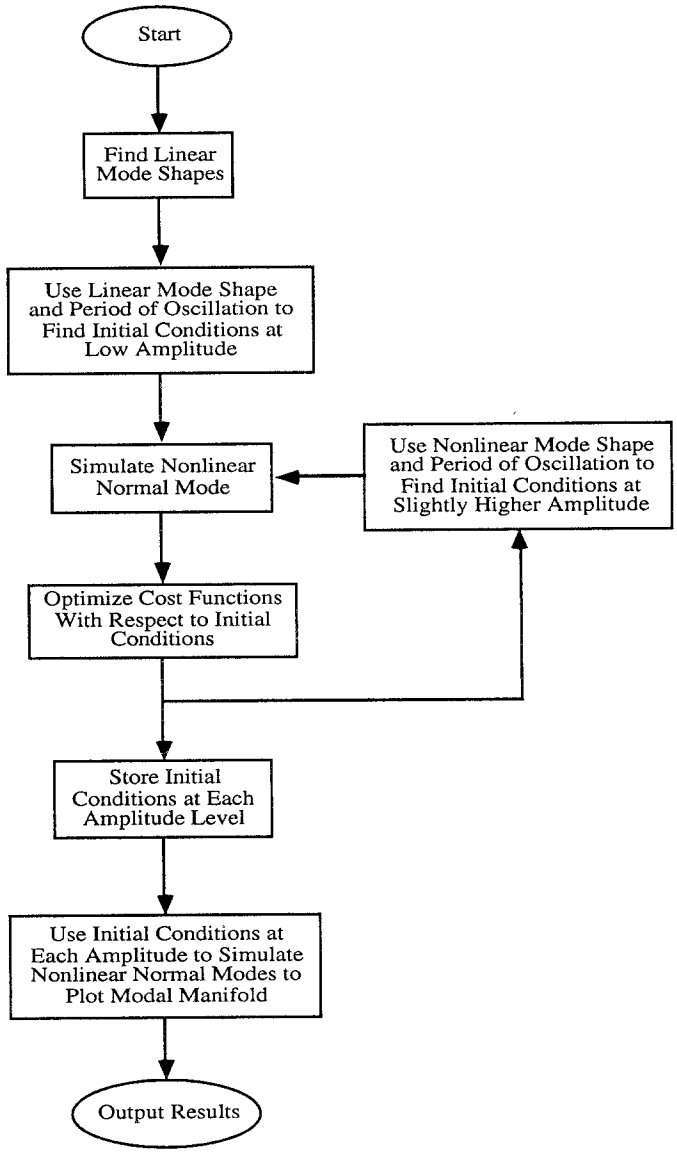

Fig. 1. Algorithm flow chart.

method to modes involving repetitive motions, i.e. undamped non-gyroscopic systems. By expressing the deviation of the motion from the definitions, a cost representing distance from a nonlinear modal manifold is found. Optimization tools are then used to minimize this cost, and thus numerically determine the shape of the nonlinear manifold.

Numerical Determination of the Nonlinear Normal Modes

Determination of the nonlinear normal mode shapes can be broken down into five steps, many of which are repeatedly performed in the identification process (see Figure 1). The first step of this approach is the determination of the linear modes of the linearized system. As in perturbation theory, it is assumed here that the nonlinear normal modes exist near the linear

modes of the linearized system. However, this constraint must only be met at the starting point of the optimization process. By choosing the starting point to be at a sufficiently low amplitude, this condition can always be met. The initial states of the system are chosen such that the system is moving on or close to only one mode. This provides the starting point for the determination of the selected nonlinear normal mode. Each nonlinear normal mode is then identified one mode at a time from a similar starting point.

The second step is the integration of the nonlinear equations forward one period of oscillation (as approximately by one period of the linear system) from an initial condition of zero displacement and initial velocities placing the motion on the linear mode of choice. The equations are also integrated backward from the same initial condition. This creates approximately two cycles of motion near the nonlinear normal mode. Both the period of oscillation and the path of the motion in the trajectory space will be in error. If the chosen initial condition causes the motion to be identically repeated, then the motion has taken place in a nonlinear normal mode [7]. If the final displacements are non-zero after integrating forward one cycle, then the motion is either not taking place in a nonlinear normal mode or the period of oscillation is incorrect.

The third step is the determination of a measure of error for the chosen initial conditions. Two measures of error are readily apparent. The first is

$$\text{cost}_1 = \sum_{i=1}^{2n} \left(\int_0^{\tau} (z_i(t) - z_i(t-\tau))^2 \, \mathrm{d}t \right), \tag{1}$$

where z_i represents the ith state when the equations are written in state space, t represents time, τ represents the approximate period of oscillation, and n is the number of degrees of freedom. This measure quantifies how far apart the two successive cycles are from each other. A second simpler measure of error is given by

$$\text{cost}_2 = \sum_{i=1}^{n} x_i(\tau)^2, \tag{2}$$

where x_i represents the ith displacement, which measures variation of the displacement after a period τ.

The fourth step in determining the nonlinear normal modes is the minimization of these errors. Minimization of the first cost function such that its value is zero is identical to meeting the Rosenberg [7] criteria for a nonlinear normal mode when τ is known. Unfortunately, the true period of oscillation, τ^*, is not known *a priori*. It is approximately known, however, since it is nearly identical to the linear period of oscillation for small oscillations. The minimum value for each cost function is zero when the system is moving in a nonlinear normal mode and $\tau = \tau^*$. Practical limitations of numerical integration dictate that zero values for the cost functions are most likely unobtainable. The best approximation for the nonlinear normal mode and its period of oscillation is the trajectory, found from integration of the nonlinear state equations of motion, that minimizes both costs. Since the minimums for functions one and two may not occur at the same place, a linear combination of the two functions is minimized instead.

An infinite number of solutions exist to the minimization problem unless the modal amplitude is constrained in some fashion. This can be done by constraining the kinetic energy at time zero to be constant throughout the optimization, or by constraining one single velocity

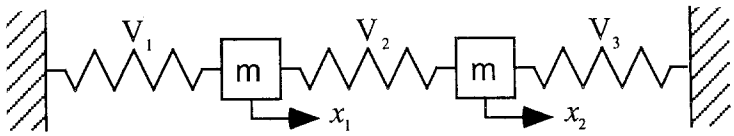

Fig. 2. A nonlinear two-degree-of-freedom system.

to a constant at time zero. This later constraint can fail, however, in the case where the chosen degree of freedom is near a linear node [1], or when mode localization takes place. Once the initial values for the velocities have been determined for a low amplitude motion of the system in the selected mode, then the nonlinear mode shape is identified for that single level of vibration.

The final step is to use the initial values found for the low amplitude of vibration, increase them by a small step (perhaps 10%) and combine them with the determined value of τ^* for the previous amplitude as the initial guesses for the optimization at a slightly higher modal amplitude. If the step size is small enough, the initial guess will be close enough to allow quick minimization of equations (1) and (2). If the step size is too large, the initial conditions will be sufficiently far away from the desired mode such that another minimum of equations (1) and (2) may be found pertaining to one of the other modes.

Steps two through five are repeatedly performed until a set of initial conditions and corresponding periods of oscillation are found over the range of modal amplitudes desired for the chosen model. All of the preceding steps are then performed for each desired nonlinear normal mode.

Example

Consider the two-degree-of-freedom system studied by Shaw and Pierre [9] shown in Figure 2. The potential energies of the springs are given by

$$\begin{aligned} V_1 &= \frac{1}{2}x_1^2 + \frac{1}{8}x_1^4 \\ V_2 &= \frac{1}{2}(x_2 - x_1)^2 \\ V_3 &= \frac{1}{2}x_2^2 \end{aligned} \tag{3}$$

and the masses are of unit mass. The equations of motion for the system are

$$\begin{bmatrix} \dot{x}_1 \\ \dot{y}_1 \\ \dot{x}_2 \\ \dot{y}_2 \end{bmatrix} = \begin{bmatrix} y_1 \\ -2x_1 - \frac{1}{2}x_1^3 + x_2 \\ y_2 \\ x_1 - 2x_2 \end{bmatrix}, \tag{4}$$

where y_1 and y_2 are the time derivatives of the positions x_1 and x_2. For small amplitude motion, the system can be approximated by the equations

$$\begin{bmatrix} \dot{x}_1 \\ \dot{y}_1 \\ \dot{x}_2 \\ \dot{y}_2 \end{bmatrix} = \begin{bmatrix} y_1 \\ -2x_1 + x_2 \\ y_2 \\ x_1 - 2x_2 \end{bmatrix}. \tag{5}$$

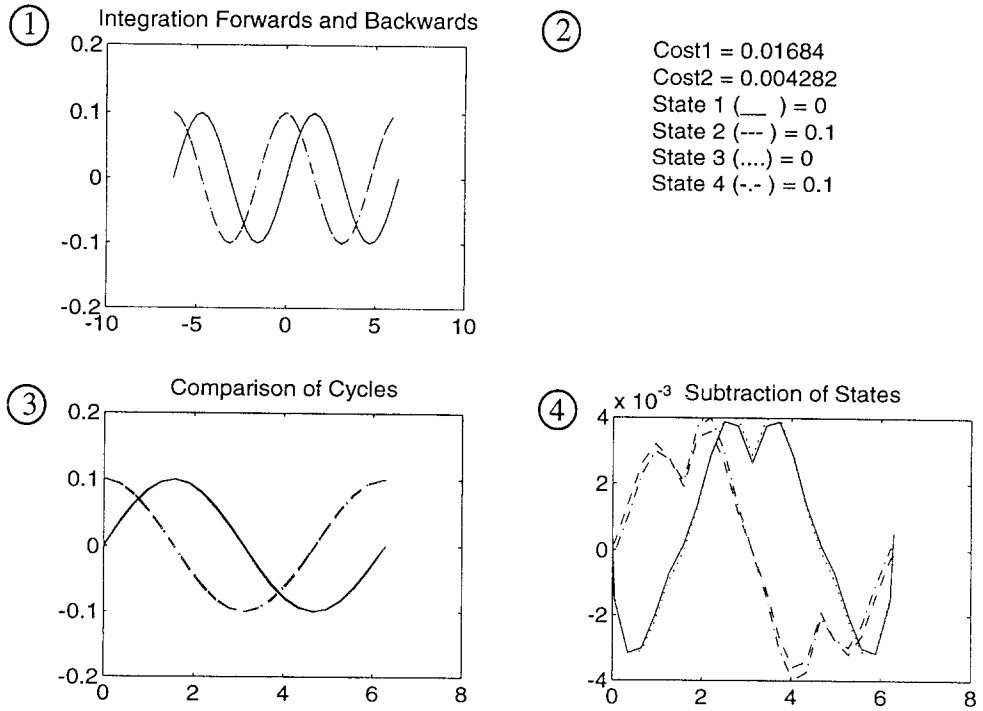

Fig. 3. Numerical results of forward integration from $[\dot{x}_1 \ \dot{y}_1 \ \dot{x}_2 \ \dot{y}_2]^T = [0 \ 0.1 \ 0 \ 0.1]^T$.

The linear mode shapes for these equations are $x_1 = x_2$ and $x_1 = -x_2$ with natural frequencies of 1 rad/sec and $\sqrt{3}$ rad/sec. For demonstration purposes, only the determination of the first nonlinear normal modes will be shown. Both nonlinear normal modes are shown in the results, however.

For small oscillations, the first nonlinear normal mode and the first linear mode will nearly coincide. Thus, initial conditions on the first linear mode will nearly coincide with initial conditions on the nonlinear normal mode. The starting guess for the initial conditions is chosen to be $[\dot{x}_1 \ \dot{y}_1 \ \dot{x}_2 \ \dot{y}_2]^T = [0 \ 0.1 \ 0 \ 0.1]^T$. The results are shown in Figure 3. Cell one is a plot of all four states integrated forward and backward in time. Cell two shows the initial conditions and the cost functions for this set of initial conditions. In cell three, the two cycles have been plotted on the same time scale for comparison. Cell four shows the differences in the states between the two cycles.

It is clear from Figure 3 that the initial conditions determined from the linear mode are very close to the nonlinear normal mode. Constrained minimization was performed using the constr.m function of the MATLAB® Optimization Toolbox. Free states of the initial conditions (the velocities) were constrained to within 20% of their initially guessed values. This constraint kept the optimization in a region dominated primarily by the chosen mode. Likewise, the total integration period was constrained to be within 20% of the initial guess for the period of oscillation in order to constrain the integration to one period of oscillation, yet allow the period to change with amplitude. In performing this example, it was also determined that cost two could be used just as effectively as a linear combination of the two costs. This slightly reduced the function evaluation time and thus decreased the time to perform the optimization.

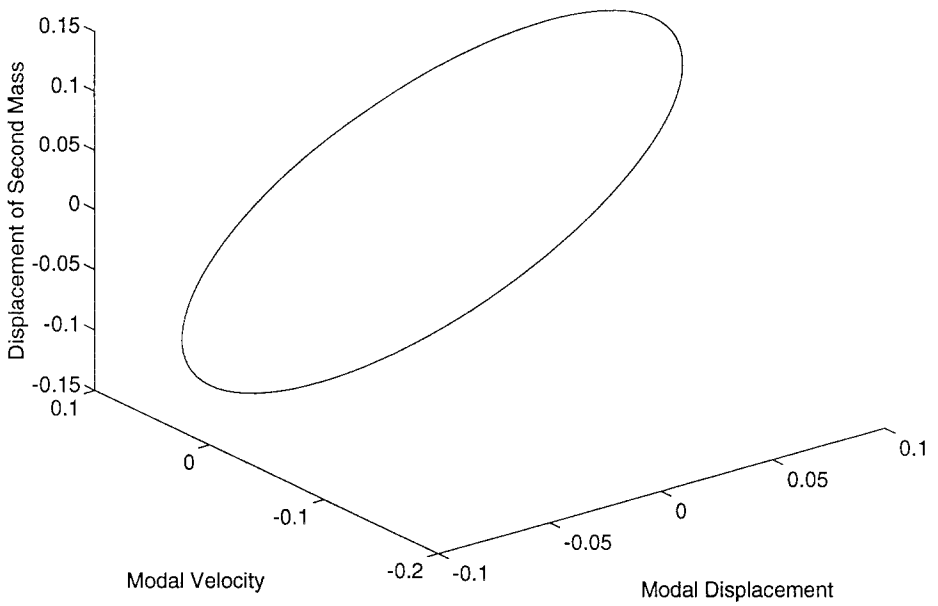

Fig. 4. Displacement of mass two as a function of the modal displacement and velocity for mode one at low amplitude.

Minimization of the total cost function yields that the actual initial conditions should be $[\dot{x}_1 \ \dot{y}_1 \ \dot{x}_2 \ \dot{y}_2]^T = [0 \ 0.10000 \ 0 \ 0.10025]^T$. Figure 4 shows the displacement of mass two as a function of the modal displacement and velocity for mode one over two cycles. (Note that for this example, the motion of the first mass has been defined as the modal coordinate.) Clearly the system is moving in the nonlinear normal mode nearest the corresponding linear mode for the initial conditions found since the modal motion is repeated.

As would be expected, at higher amplitudes the nonlinear mode shape diverges from the linear mode shape. Figure 5 shows the numerical results of forward and backward integration from $[\dot{x}_1 \ \dot{y}_1 \ \dot{x}_2 \ \dot{y}_2]^T = [0 \ 1 \ 0 \ 1]^T$. Clearly this guess for the initial condition is quite poor, but it is still closer to the first nonlinear mode than the second nonlinear mode. In stepping through initial modal velocity amplitudes from 0.1 to 1, the initial prediction for the velocity of mass two is 1.21071. The final result after minimizing the cost function is found to be 1.25790. As an example, Figure 6 shows the motion of the second mass as a function of the modal amplitude and velocity found from numerically integrating the equations of motion from the "correct" initial conditions. This result was repeated for a range of modal amplitudes from 0.1 to 2 by steps of 0.1. The results are shown in Figure 7. By stepping through to higher amplitudes gradually, the optimization at each amplitude can begin from a much better starting point, and the optimization is much more likely to converge to the correct nonlinear normal mode (and will converge much more quickly) than if larger steps are taken.

To give an idea of how nonlinear mode one is, Figure 8 shows the difference between the numerically determined nonlinear normal mode and the linear mode. It is clear that even at relatively low amplitudes, the nonlinear contribution is significant.

Shaw and Pierre [9] represented the first nonlinear normal mode with a third order polynomial in the modal displacement, u, and the modal velocity, v, as $x_2 = u + 1/6u^3 + 1/4uv^2$ where x_2 is the displacement of the second degree of freedom. Numerically solving for the first nonlinear normal mode and curve fitting u and v yields instead that $x_2 = u + 0.18780u^3 + 0.22403uv^2$.

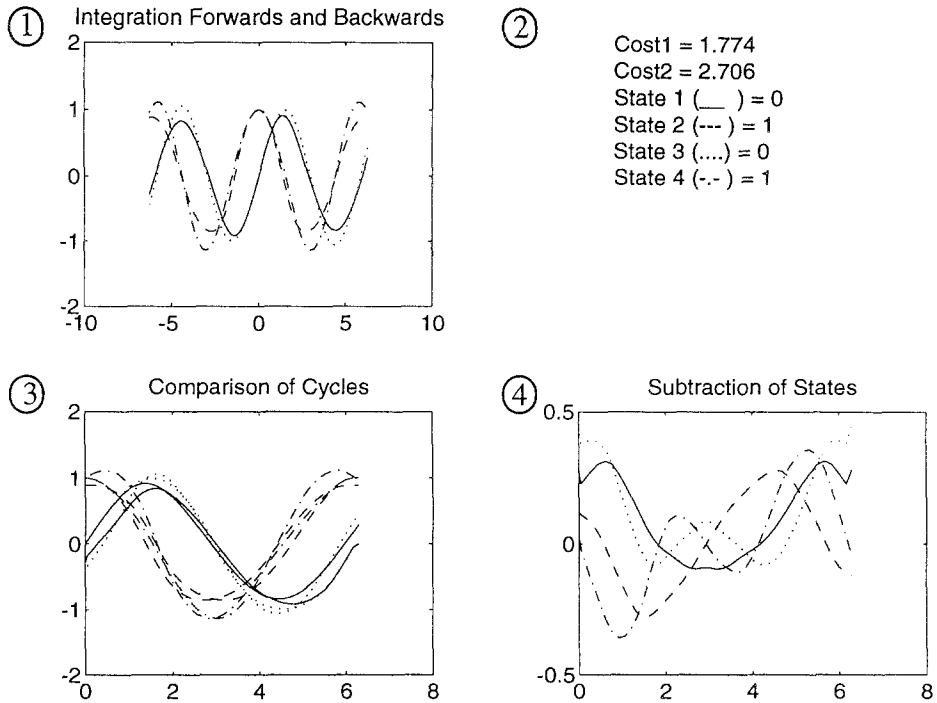

Fig. 5. Numerical results of forward integration from $[\dot{x}_1 \ \dot{y}_1 \ \dot{x}_2 \ \dot{y}_2]^T = [0 \ 1 \ 0 \ 1]^T$.

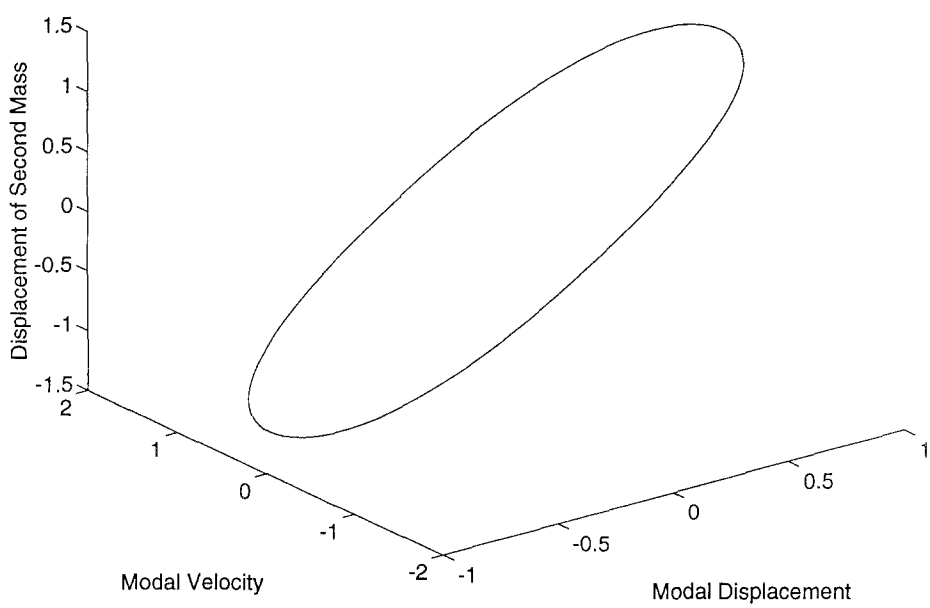

Fig. 6. Displacement of mass two as a function of the modal displacement and velocity for mode one at high amplitude.

All of the other polynomial coefficients found using the numerical method are zero to five decimal places. The error between the two polynomial representations and the numerically determined mode are shown in Figures 9 and 10.

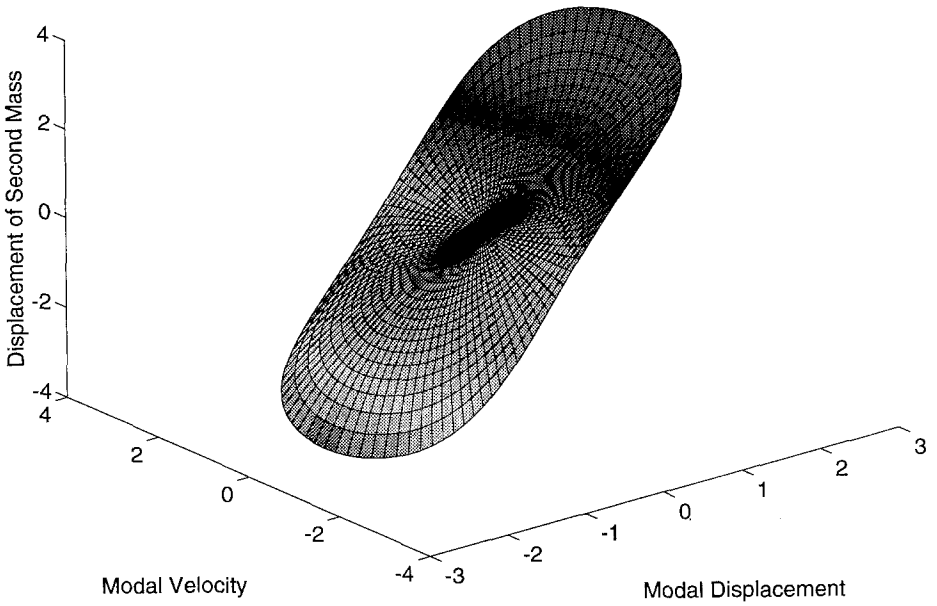

Fig. 7. Displacement of mass two as a function of the modal displacement and velocity of mode one for modal amplitudes from 0.1 to 2.

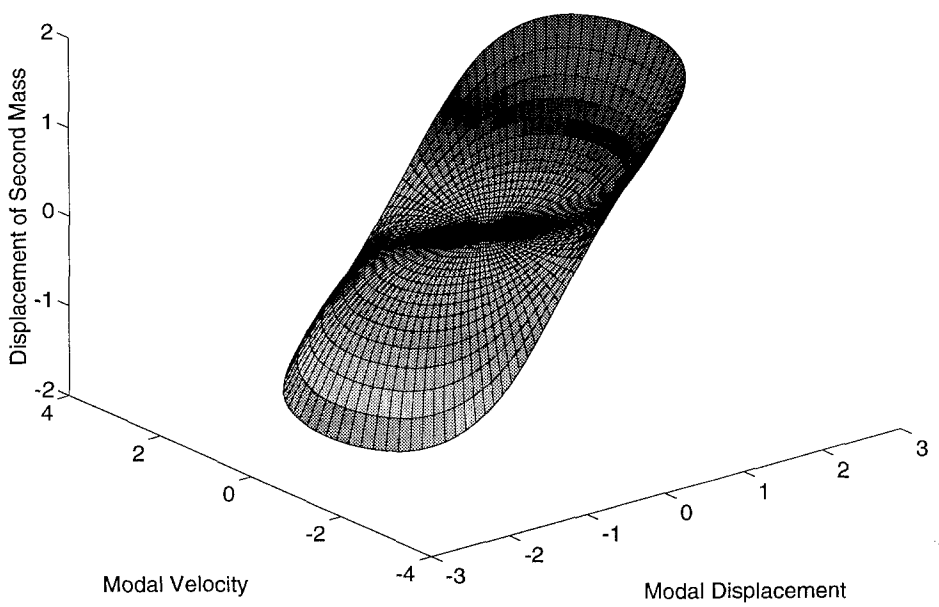

Fig. 8. Nonlinear part of the displacement of mass two as a function of the modal displacement and velocity of mode one for modal amplitudes from 0.1 to 2 (error if linear modes assumed).

Clearly, the polynomial fit of the numerical solution is a better representation of the nonlinear normal mode at higher amplitudes. This is because the invariant manifold method, not unlike perturbation methods, is dependent on relatively low amplitudes in order to have convergence of the polynomial. Above a modal amplitude of 1, the assumption that higher order polynomial terms are negligible cannot be assumed (truncation of the power series expansion cannot be justified). Thus, the analysis cannot be performed accurately. In simply

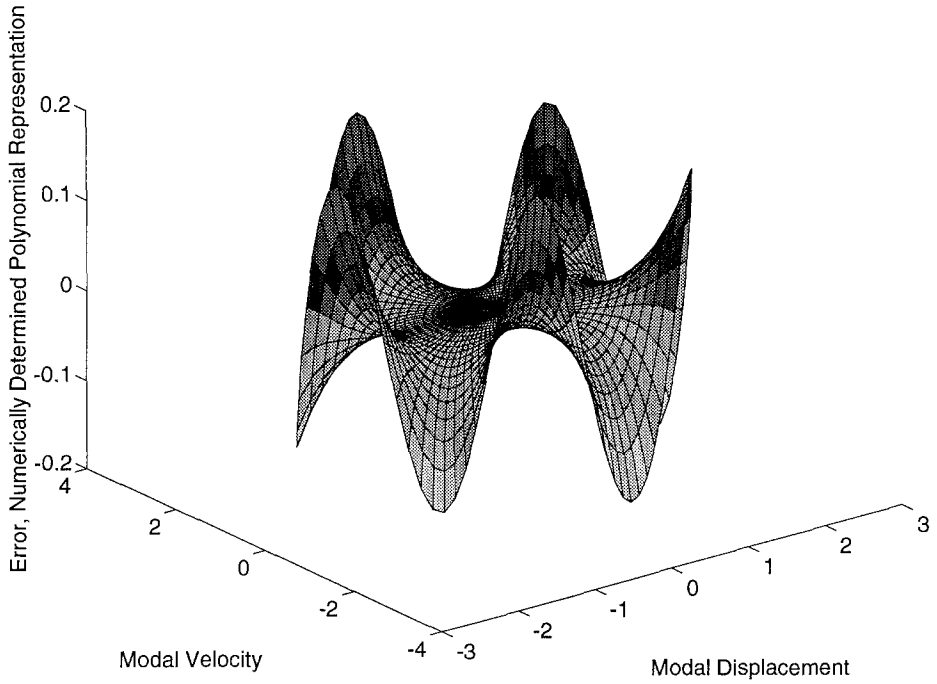

Fig. 9. Difference between numerical solution and polynomial curve fit for mode one.

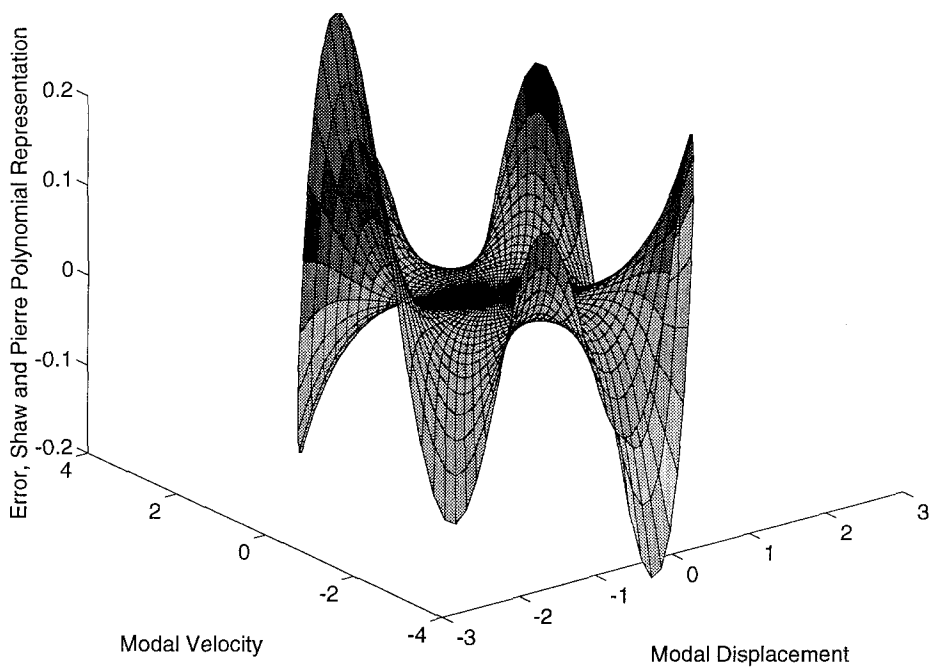

Fig. 10. Difference between numerical solution and invariant manifold solution for mode one.

curve fitting a polynomial to the raw data for the range of amplitudes of interest, a much better polynomial representation to the nonlinear normal mode can be obtained. It is also possible

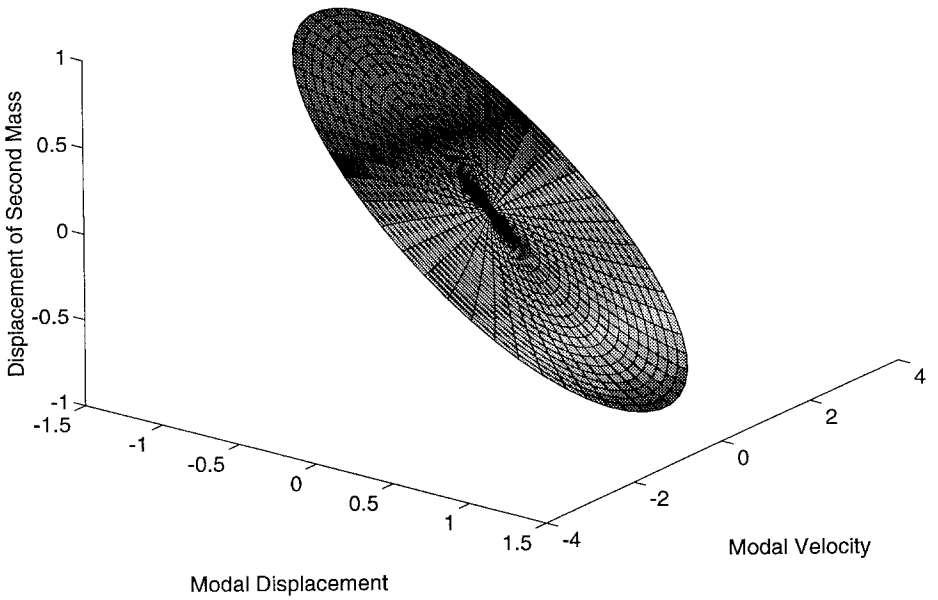

Fig. 11. Displacement of mass two as a function of the modal displacement and velocity of mode two for modal amplitudes from 0.1 to 2.

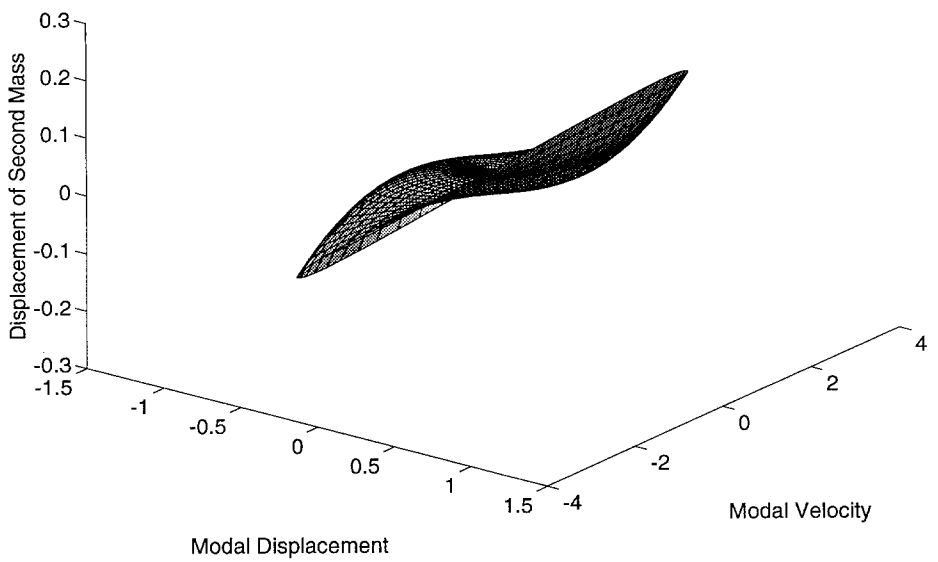

Fig. 12. Nonlinear part of the displacement of mass two as a function of the modal displacement and velocity of mode two for modal amplitudes from 0.1 to 2 (error if linear modes assumed).

to easily evaluate the accuracy of the polynomial representation by observing error plots such as Figures 9 and 10.

The second nonlinear normal mode was also determined numerically and is shown in Figure 11. It is extremely planar and thus is very close to the linear mode even at high amplitudes. Figure 12 shows the error obtained when assuming that the mode is linear. Note that the modal displacement and modal velocity axes of Figures 11 and 12 have been switched as compared to Figures 7–10 to aid in the visualization of mode two.

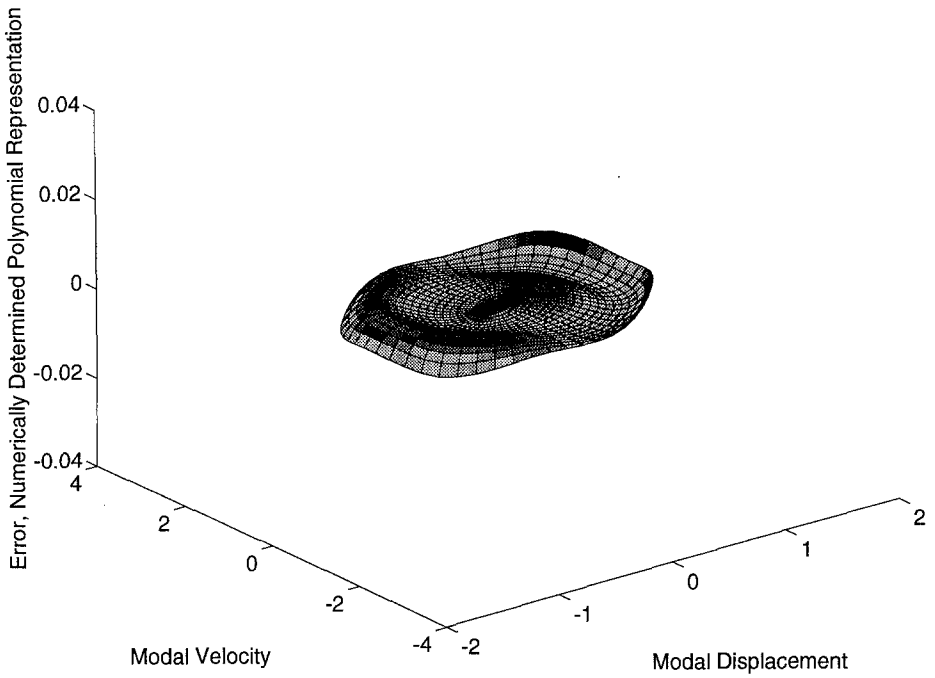

Fig. 13. Difference between numerical solution and polynomial curve fit for mode two.

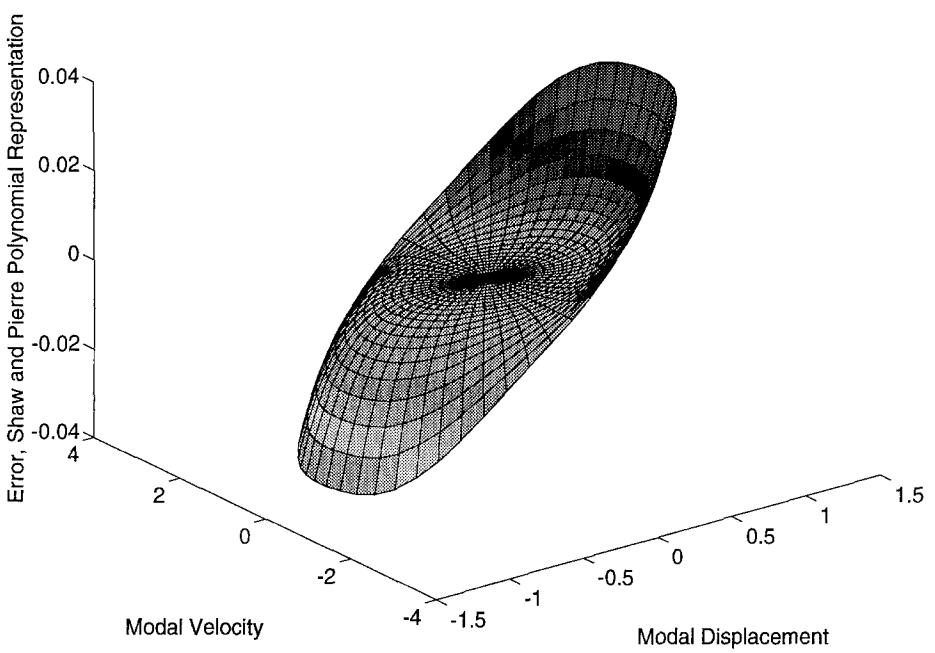

Fig. 14. Difference between numerical solution and invariant manifold solution for mode two.

Shaw and Pierre [9] represented the second nonlinear normal mode by a third order polynomial in the modal displacement, u, and the modal velocity, v as $x_2 = -u + 5/26u^3 + 3/52uv^2$ where x_2 is the displacement of the second degree of freedom. Numerically solving for the first nonlinear normal mode and curve fitting a third order polynomial in u and v

yields instead that $x_2 = -0.99117u + 0.16243u^3 + 0.04676uv^2$. All of the other polynomial coefficients found using the numerical method are again zero to five decimal places. The error between the two polynomial representations and the numerically determined mode are shown in Figures 13 and 14.

Again, the polynomial curve fit of the numerically determined nonlinear normal mode is much more accurate at high amplitudes than the representation determined using the invariant manifold method. It should be noted however that both representations are always less than 5% away from the numerically determined solution for the range of amplitudes considered for mode 2.

Conclusion

A numerical method for determining nonlinear normal modes has been presented that allows for greater accuracy at high amplitudes than analytical methods that rely on power series expansions. This is due to the effect that power series cannot be effectively truncated at higher amplitudes. An example has been presented that demonstrates the breakdown of power series representations at high amplitudes while demonstrating the ability to numerically identify the mode shapes. Although the numerical method can be used to find nonlinear normal modes more accurately, it is clear from the flow chart of Figure 1 that in cases where bifurcation occurs, the bifurcation can go undetected if it is not identified *a priori.*

References

1. Boivin, N., Pierre, C., and Shaw, S. W., 'Non-linear normal modes, invariance, and modal dynamics approximations of non-linear systems', *Nonlinear Dynamics* **8**, 1995, 315–346.
2. Caughey, T. K., Vakakis, A. F., and Sivo, J., 'Analytical study of similar normal modes and their bifurcations in a class of strongly non-linear systems', *International Journal of Non-Linear Mechanics* **25**, 1990, 521–533.
3. King, M. E. and Vakakis, A. F., 'An energy-based formulation for computing nonlinear normal modes in undamped continuous systems', *Journal of Vibration and Acoustics*, in press.
4. Manevich, L. I. and Mikhlin, Iu. V., 'On periodic-solutions close to rectilinear normal vibration modes', *Soviet Journal of Applied Mathematics and Mechanics (PMM)* **36**(6), 1972, 1051–1058.
5. Nayfeh, A. H. and Mook, D. T., *Nonlinear Oscillations*, John Wiley & Sons, New York, 1979.
6. Nayfeh, A. H. and Nayfeh, S. A., 'Nonlinear normal modes of a continuous system with quadratic nonlinearities', *Journal of Vibration and Acoustics* **117**, 1995, 199–205.
7. Rosenberg, R., 'On non-linear vibrations of systems with many degrees of freedom', in *Advances in Applied Mechanics*, Vol. 9, G. Kuerti (ed.), Academic Press, New York, 1966, pp. 155–242.
8. Shaw, S. W., 'An invariant manifold approach to nonlinear normal modes of oscillation', *Journal of Nonlinear Science*, **4**(9), 1994, 419–448.
9. Shaw, S. W. and Pierre, C., 'Normal modes for nonlinear vibratory systems', *Journal of Sound and Vibration* **164**(1), 1993, 85–124.
10. Shaw, S. W. and Pierre, C., 'Normal modes of vibration for nonlinear continuous systems', *Journal of Sound and Vibration* **169**(3), 1994, 319–347.
11. Shaw, S. W. and Pierre, C., 'On nonlinear normal modes', in *Proceedings of the Winter Annual Meeting of the A.S.M.E.*, Anaheim, California, November 1992, DE-Vol. 50, AMD-Vol. 144, pp. 1–5.
12. Vakakis, A., 'Analysis and identification of linear and nonlinear normal modes in vibrating systems', Ph.D. Thesis, California Institute of Technology, 1990.
13. Vakakis, A. F. and Cetinkaya, C., 'Mode localization in a class of multidegree-of-freedom nonlinear systems with cyclic symmetry', *SIAM Journal of Applied Mathematics* **533**, 1993, 265–282.
14. Vakakis, A. F. and Rand, R. H., 'Normal modes and global dynamics of a two-degree-of-freedom non-linear system – Low energies', *International Journal of Non-Linear Mechanics* **27**, 1992, 861–874.
15. Vakakis, A. F. and Rand, R. H., 'Normal modes and global dynamics of a two-degree-of-freedom non-linear system – High energies', *International Journal of Non-Linear Mechanics* **27**, 1992, 875–888.